# Microanatomic characteristics of the insertion of the distal sesamoidean impar ligament and deep digital flexor tendon on the distal phalanx in healthy feet obtained from horses

Kimberly K. Van Wulfen, DVM, MS, and Robert M. Bowker, VMD, PhD

**Objective**—To describe microanatomic characteristics of the insertion of the distal sesamoidean impar ligament (DSIL) and deep digital flexor tendon (DDFT) on the distal phalanx in horses.

**Sample Population**—Healthy feet obtained from 62 horses of various breeds.

**Procedure**—Feet from 23 horses were used to histologically examine the insertion of the DSIL and DDFT (n = 7), its vasculature (10), and neural elements (6). In 39 other horses, the insertion zone was examined for proteoglycan.

**Results**—The insertion of the DSIL and dorsal half of the DDFT contained bundles of collagen fibers with intervening loose connective tissue septa with arteriovenous complexes (AVC) and nerve fibers. Microscopic examination revealed adaptive changes in the insertion with regard to proteoglycan content. In young adult horses, little or no staining for proteoglycans was evident, whereas in middle-aged horses, moderate proteoglycan staining was seen. Six older horses had slight proteoglycan staining at the insertion.

**Conclusions and Clinical Relevance**—The study revealed that this region contained a rich neurovascular complex between the collagen bundles. A gradual increase in production of proteoglycan, evident at the insertion of the DSIL and DDFT on the distal phalanx, indicates that adaptive responses to stress rather than age alone may be the primary determining factor. These observations indicate that this insertion site may be susceptible to stress during stance and impact loading, because this region appears to be strategically situated to regulate important neurovascular functions of the foot. (*Am J Vet Res* 2002; 63:215–221)

The continued success of any performance horse is dependent on its feet being free of any lameness conditions. Many lameness problems associated with structures in the palmar aspect of the foot include degenerative diseases of the **distal interphalangeal (DIP)** joint, ringbone, fractures of the distal phalanx and navicular bone, bruises, and septic infections.[1] Whereas the actual causes of many conditions may be generally known, one condition (ie, navicular syndrome) remains ambiguous in terms of the initiating causes or pathogenesis, even though the problem has been documented and discussed for more than 200 hundred years.[2-4] Several hypotheses have been proposed for the pathogenesis of this condition, including biomechanical effects attributable to pressure of the **deep digital flexor tendon (DDFT)** against the navicular bone, vascular insults with partial arterial blockage to the navicular bone, and increases in bony remodeling. Each hypothesized idea has been discussed thoroughly, using analyses of clinical, radiographic, and pathologic findings. Histologic findings of the navicular bone are in general agreement with the hypothesis that this bone undergoes extensive remodeling as a result of this chronic condition.[2-5] However, each proposed hypothesis focuses on the navicular bone as the important primary initial point from which the pathogenic processes and clinical signs of pain emanate. Few reports have considered the possibility that other regions of the foot may be involved in the early pathogenic processes, which will potentially affect the navicular bone secondarily. As a result, other important observations may have been overlooked in the formulation of these hypotheses. For example, the findings that pressure against the navicular bone does not vary significantly among gaits[6,7] and that the strain in the DDFT decreases prior to maximum loading of the limb and breakover at the toe[8] may argue against the causal hypothesis that emphasizes high DDFT pressure against the navicular bone as a prime factor in navicular syndrome. The relative lack of thrombi in vessels argues against vascular occlusion as a major factor.[2-4] One potentially overlooked region of the foot that we believe may be critical in the initial pathologic processes associated with this chronic debilitating condition is the insertion of the **distal sesamoidean impar ligament (DSIL)** and DDFT on the distal phalanx and their associated connective tissues on the flexor surface of the distal phalanx. This zone on the distal phalanx extends from the semilunar line and the more proximal roughened insertion areas encompassing the 2 solar foramen located abaxial to the articulation between the navicular bone and distal phalanx.

Although the DSIL and DDFT are generally believed to have a structure and function similar to that of other ligaments and tendons near the insertions onto bone, our preliminary observations[9] suggested that this insertion region and its tissues differ in basic structure from that described in other reports on liga-

Received May 1, 2001.
Accepted Aug 9, 2001.
From the Department of Pathobiology and Diagnostic Investigation, College of Veterinary Medicine, Michigan State University, East Lansing, MI 48824.
Supported in part by the American Quarter Horse Association.
This manuscript represents a portion of a thesis submitted by the senior author to the Michigan State University Graduate School as partial fulfillment for the requirements of a Master of Science degree.
Address correspondence to Dr. Bowker.

ments and tendons; this basic difference may contribute to the initial pathogenesis of navicular syndrome. Thus, the purpose of the study reported here was to examine the microanatomic and histochemical characteristics of this region in healthy feet of horses in terms of functional morphology. We believe that results of this study may begin to provide a basis for our understanding of the potential contributions to the pathogenesis of navicular syndrome.

## Materials and Methods

**Sample population**—Feet were obtained from 23 horses submitted to the Animal Health Diagnostic Laboratory at Michigan State University. Horses represented various breeds and their crosses, including Standardbreds (n = 7), Quarter Horses (6), Arabians (5), Appaloosas (3), and Thoroughbreds (2). The horses ranged from < 1 year to 30 years old. All horses had healthy feet and did not have a history of chronic foot problems as indicated by the owners, referring veterinarians, or clinicians at our facility.

Feet also were obtained from an additional 39 horses (Standardbreds [n = 9], Quarter Horses [9], Thoroughbreds [4], Arabians [3], and undetermined miscellaneous breeds and crossbred horses [14]). These horses ranged from 2 to 29 years old. None of them had a history of lameness or foot problems, and the feet appeared healthy during examination. These horses were primarily used for pleasure riding 1 to 5 times/wk during the warmer months, although 3 of the Standardbreds had recently been in training for harness racing.

After horses were euthanatized, 1 forefoot was randomly removed from each horse. Feet were obtained from the right and left side with the ipsilateral fore- and hind limbs obtained from each of the 62 horses.

**Macroscopic anatomy and histologic examination**—In the first portion of the study, 23 feet from the initial horses were allocated into 3 groups for this study (10 feet were perfused with India ink, 7 feet were processed for routine histologic examination, and 6 feet were processed to enable assessment of neural structures). Immediately after the horses were euthanatized, 10 feet were harvested, and the vasculature of each foot was flushed with 300 to 500 ml of warm physiologic saline (0.9% NaCl) solution. The vasculature then was perfused with India ink, using an infusion of 120 ml of a solution of 30% India ink and 5% gelatin in 0.1*M* sodium phosphate buffer (pH 7.4). This solution was infused manually via the medial palmar artery (7 feet) or the dorsolateral metatarsal artery (3 feet), using a 60-ml syringe. All vessels were ligated at the proximal aspect of the metacarpus (or metatarsus) to prevent loss of the perfusate, and the final 30 to 40 ml of the India ink solution was infused under pressure to maximize filling of the vasculature. The feet then were placed in an upright position in a freezer at –10 to –15 C for several days to 1 week.

Feet were removed from the freezer, cut into parasagittal sections (thickness of 0.5 to 0.7 cm) on a band saw, and placed in buffered formalin. After 24 hours, tissues in the area of the DSIL-DDFT insertion were removed and placed into a sequential series of gelatin solutions that ranged in concentration from 10 to 25%. After soaking in these solutions at 36 C for 12 to 24 hours, the tissues were subsequently embedded in a solution of 25% gelatin and chilled at 4 C, after which the tissue was suspended within a gelatin block that was then placed in a solution of 5% formalin for 24 hours to solidify and fix the gelatin. Gelatin blocks were sectioned on a freezing microtome at a thickness of 90 µm; sections were collected serially and mounted on electrically charged slides to minimize curling. The slides then were dried and routinely counter stained.

In a second portion of the study, a band saw was used to cut 7 feet into parasagittal sections or sections parallel to the ground (thickness, 0.5 to 0.7 cm). Sections were examined macroscopically for signs of pathologic changes in the navicular bone and its ligaments, including synovial fossae in the navicular bone, adhesions between the navicular bone and DDFT, erosions of the flexor cortex, or longitudinal grooves in the dorsal surface of the DDFT. Sections then were placed in a solution of 10% formalin buffered with sodium phosphate (pH 7.2 to 7.4) for 2 days to 1 week. The area of the insertion of the DSIL-DDFT on the distal phalanx, **collateral sesamoidean ligament (CSL)**, DDFT at the flexor surface of the navicular bone, and DDFT at the level of the CSL were isolated, and samples were routinely processed for histologic examination (6-µm-thick sections), using H&E stain as well as van Gieson stain for elastic fibers, prior to application of a coverslip. In selected feet, the straight sesamoidean ligament, collateral ligament of the DIP joint, and oblique sesamoidean ligament were processed in a similar manner. In these sections of the other ligaments within the digit, the patterns of organization of collagen fibers and possible septa were examined. Tissue sections from the aorta served as control samples for staining of elastic fibers.

In 6 feet, fresh tissue samples were obtained from the area of the insertion of the DSIL-DDFT on the distal phalanx. These tissues were impregnated with gold chloride, as described by Zimny et al,[10] and used to identify neural elements within the region of the insertion.

In the third portion of this study, forefeet obtained from the latter 39 horses were cut into 6 to 8 parasagittal sections (thickness of 0.5 to 0.7 cm) and examined for macroscopic signs of injury or pathologic changes. Each series of sections was examined closely by use of a low-power (10 to 15X) dissecting microscope with emphasis placed on potential macroscopic changes in the navicular bone and its associated structures.

Tissue sections then were placed in sodium phosphate-buffered formalin (pH 7.4). The insertion of the DSIL and DDFT on the distal phalanx and palmar half of the DIP joint (articulation between the distal phalanx and entire navicular bone) were removed as a single block and gradually decalcified in 20% formic acid during a 2-week period. Tissues were tested for complete decalcification prior to embedding in paraffin. Tissue sections were cut at a thickness of 6 µm and counter stained with safranin O dye and fast green (3 to 5 sections) and H&E (2 to 4 sections) prior to examination by use of light microscopy. Safranin O and fast green stains were used to identify fibroblasts capable of producing proteoglycans, which were evident as bright-red structures beginning around the perimeter of the nucleus and appearing to extend throughout the cell and into the extracellular matrix.

Staining patterns for proteoglycans were subjectively graded into 3 categories: little or no staining was evident, and stained fibroblasts were within a short distance (200 µm, as measured by use of an ocular micrometer) from the tidemark or the insertion site on the distal phalanx; moderate proteoglycan staining of fibroblasts that extended along the insertion site of the DSIL and DDFT as well as up to 1 mm from the tidemarks of the DSIL and DDFT; and an extensive area of staining that extended along the entire insertion of the DSIL and DDFT as well as extending more than 1 mm proximally along the DSIL and DDFT from the tidemark. A greater population of cells and surrounding extracellular matrix were stained for proteoglycans in the second category, compared with the first category.

## Results

The distal aspect of the navicular bursa and surrounding structures was examined on parasagittal sec-

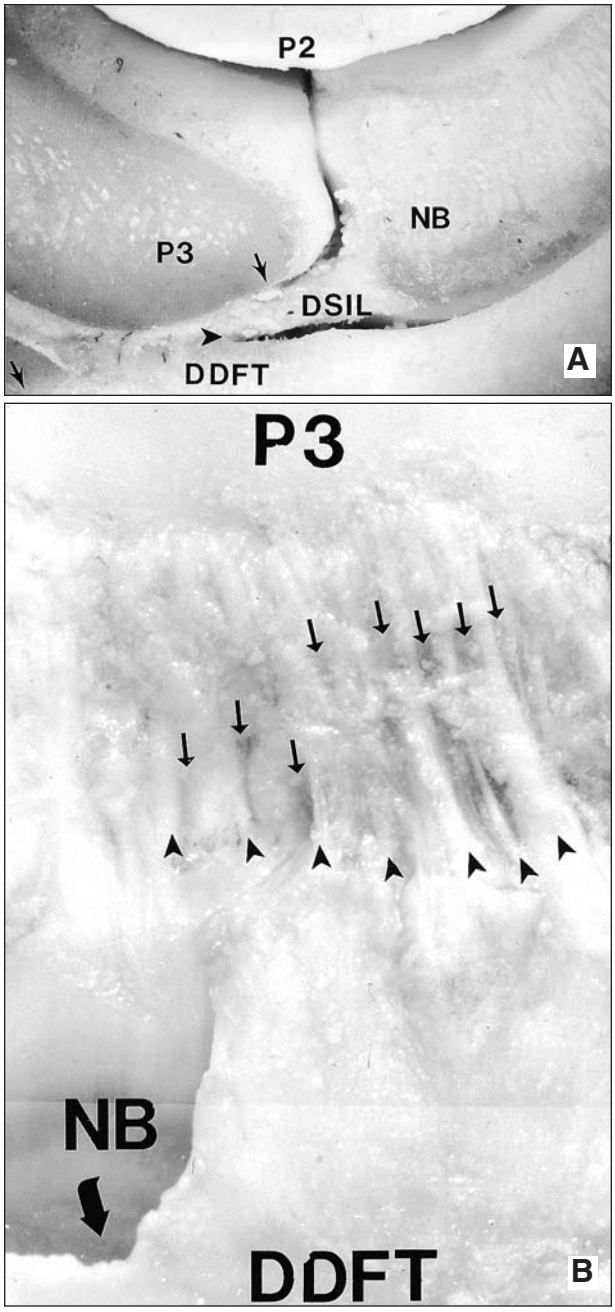


Figure 1—Low-magnification photographs of a parasagittal section (A) and a section cut parallel to the surface of the ground (B) from the healthy feet of horses, revealing the insertion of the deep digital flexor tendon (DDFT) and distal sesamoidean impar ligament (DSIL) on the distal phalanx (P3). In panel A, notice at the area of the insertion (arrows) that the navicular bursa (NB) often does not extend to the distal phalanx (arrowhead). In panel B, the navicular bursa (large arrow) is between the DDFT and navicular bone. Notice that the collagen bundles (arrowheads) can be seen at the insertion for the fusion of the DDFT and DSIL along with connective tissue septa (small arrows) containing the microvasculature and sensory nerve fibers. P2 = Middle phalanx. P3 = Distal phalanx. NB = Navicular bone.

tions of the foot by displacing the DDFT palmarly from the navicular bone. The DSIL and dorsal surface of the DDFT formed the distal extent of the navicular bursa. At this site, thin connective tissue septa extended between the DSIL and DDFT to form finger-like evagi-

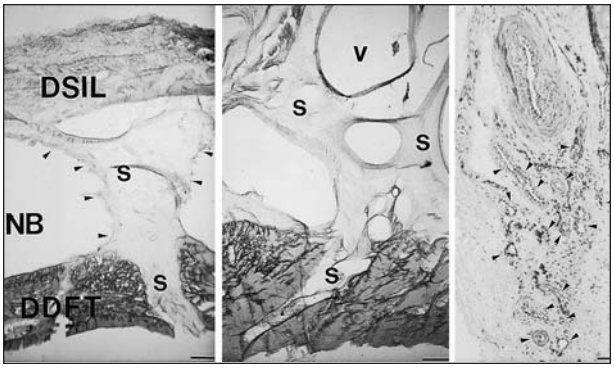


Figure 2—Photomicrographs of tissue sections in the region of the insertion of the DSIL and DDFT on the distal phalanx. Left panel—Distal outpocketings of the navicular bursa (NB) between the DSIL and DDFT are separated by thin sheets of connective tissue septa (S). The septa extend from the DSIL into the dorsal half of the DDFT (arrowheads). Middle panel—In this section obtained near the distal phalanx, notice that more small vessels (V) are evident within the septa (S). Right panel—This section was obtained from the same area as that in the middle panel. Notice that many more microvessels with arteriovenous complexes (AVC; arrowheads) are apparent within the septal sheets. The left and middle panels were not stained, and the right panel was stained with trichrome stain.

nations of the navicular bursa synovial lining near the insertions onto the distal phalanx. The connective tissue sheets between the DSIL and DDFT precluded, in most instances, full extension of the navicular bursa to the bony surface of the distal phalanx (**Fig 1**). Beyond the synovial lining of the navicular bursa and DIP joint, areolar connective tissue joined the abaxial boundaries of the DSIL and DDFT as they inserted on the distal phalanx. In sections through the insertion, the DSIL and dorsal half of the DDFT consisted of distinct, nearly parallel bands of collagen bundles with areolar tissue comprising the width of the septa (1 to 2 mm) as well as extending to the dorsal half of the DDFT. Macroscopically, the septal tissue appeared to contain many small blood vessels, as indicated by the red coloration of the fresh tissue and the fact that India ink preparations of the septa were completely black.

Histologic examination of sections allowed for a more detailed evaluation of the morphology of the DSIL-DDFT insertion. A septal sheet between the DSIL and DDFT was seen between 2 synovial evaginations of the navicular bursa (**Fig 2**). Near the distal phalanx, more microvessels were apparent within the septal sheet. The microvessels were evident in greater detail on routine histologic examination of sections of this region. When serial sections of this region were examined microscopically after infusion with India ink, the extensive microvasculature became evident as small black vessels (arterioles, venules, and capillaries), and **arteriovenous complexes (AVC)** contrasted with the clear or lightly colored connective tissue of the DSIL and DDFT. Most of the AVC were up to 1mm in diameter (range, 0.5 to 1.4 mm), and the same vascular complex could be followed through 3 to 8 serial 90-µm sections. The vascular column of India ink was observed passing from a large, thick-walled vessel into a tortuous, coiled capillary network prior to entry into a larger, thin-walled vessel (**Fig 3**). This capillary network did not branch out to supply the surrounding tis-

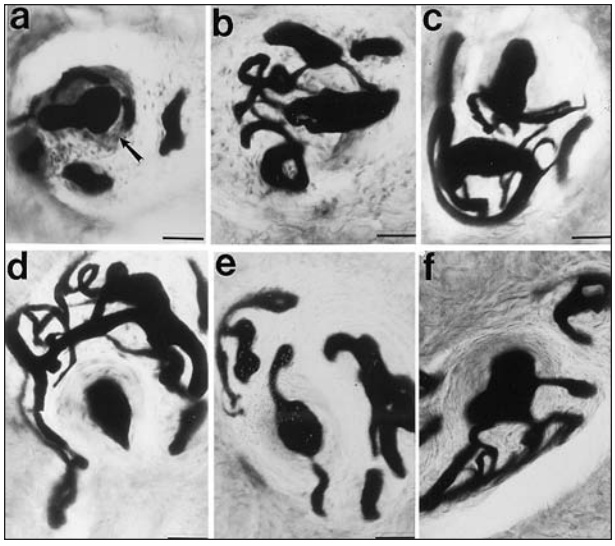


Figure 3—Photomicrographs of serial tissue sections (90-µm thick) in the regions of the DSIL-DDFT insertion on the distal phalanx from a healthy foot of a horse, revealing the typical AVC after infusion of vasculature with India ink. In the initial section (a), India-ink filled vasculature can be traced from the central vessel (a; arrow) through a tortuous capillary network, (b through d, especially c and d), and then to the point where it joins a large central vessel (e and f). Stain = H&E. Bars = 80 µm.

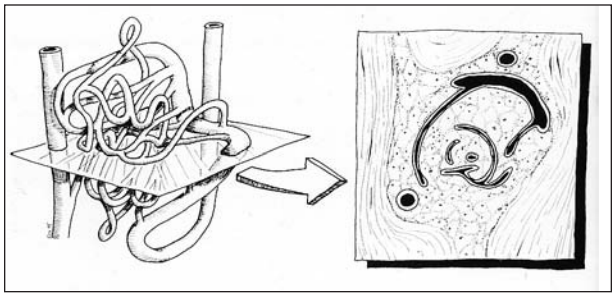

Figure 4—Diagrammatic representation of a typical AVC (left) and the appearance of the AVC in a histologic section (right).

sue but formed a glomus-type structure that was surrounded by epithelial-like cells. These complexes were seen only in the region of the insertion of the DSIL and DDFT on the distal phalanx and were not evident in the DDFT proximally at the level of the flexor cortex, at a level proximal to the navicular bone, or in the CSL. The AVC were evident in serial sections of the DSIL-DDFT insertion (**Fig 4**).

A rich neural network within the septa was identified, using the gold chloride impregnation technique. Axons commonly existed in bundles coursing through the septa of the DSIL-DDFT. In other parts of the DDFT (ie, at the level of the flexor cortex and the level proximal to the navicular bone), only a few isolated nerve fibers were seen between tendon fibers. Few nerve fibers were evident at these proximal levels in contrast to those seen in the DSIL-DDFT insertion.

The elastic composition of the connective tissue of the DSIL-DDFT insertion was evaluated and compared with connective tissues in the DDFT and other ligaments (straight sesamoidean ligament, oblique sesamoidean ligament, and collateral [medial] ligament of the DIP joint) within the equine digit. The comparative assessment could be made, because these tissues were stained concurrently, using histologic sections from the aorta as the control tissue for elastic composition. The DSIL-DDFT insertion contained prominent bundles of elastic fibers that were evident within the septa in association with the microvasculature (**Fig 5**). These elastic fibers were more abundant within the insertion than was observed in the DDFT proximally at the navicular bone and DIP joint. Elastic fibers were not common in the other sesamoidean ligaments of the digit; elastic fibers were only detected in the CSL.

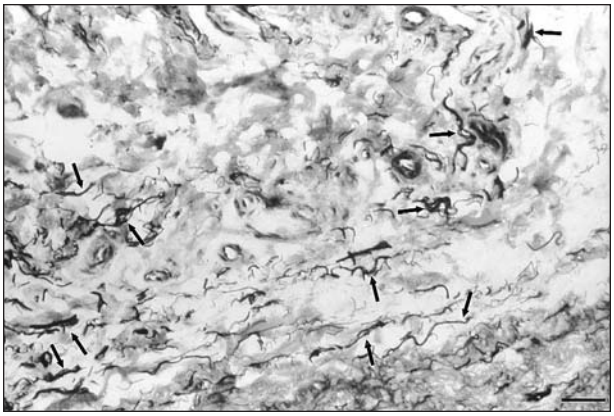

Figure 5—Photomicrograph of a tissue section obtained in the region of the DSIL-DDFT insertion on the distal phalanx revealing bundles of elastic fibers (arrows) within the septal sheets. Stain = van Gieson. Bar = 100 µm.

Additional detailed examination of the insertion of the DSIL and DDFT on the distal phalanx was undertaken in 39 feet, using H&E, safranin O, and fast green stains. Four zones of transition were recognized between the DSIL-DDFT and distal phalanx on most sections as the collagen fibers approached the flexor surface of the distal phalanx at the insertion: the distal phalanx (ie, bone), a mineralized fibrocartilage region, a fibrocartilage zone, and the distal ends of the DSIL and DDFT. The distal phalangeal bone revealed haversian systems along the insertion sites that gradually formed trabeculae at deep levels on the distal phalanx. In the insertion zone, the bone often became irregular rather than smooth (**Fig 6**). The mineralized fibrocartilage zone varied in thickness from being barely detectable to > 300 µm. A prominent tidemark line was usually seen between the mineralized fibrocartilage and nonmineralized fibrocartilage. This line delineated the outer limit of the mineralized region of the insertion of the DSIL and DDFT.

Staining characteristics of these zones were observed in each breed of horse represented, but the extent of cellular staining of proteoglycans of the DSIL and DDFT insertion on the distal phalanx was not constant. It varied considerably among the samples examined, ranging from sections that did not have proteoglycan staining to other sections that had proteoglycan staining of numerous cells as well as the extracellular matrix. In 5 samples, only staining of the DSIL was evident, whereas in 6 other samples, only the insertion of the DDFT was stained. However, in the remainder of the samples, both the DSIL and DDFT were stained.

Sections that had little or no evidence of proteo-

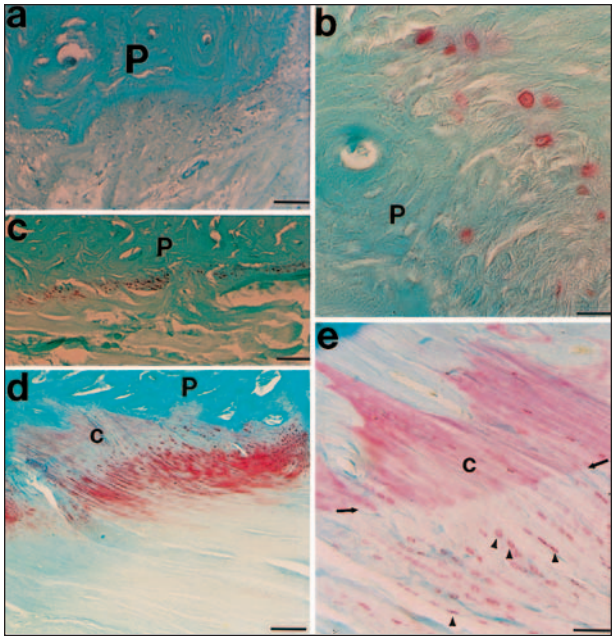


Figure 6—Photomicrographs of tissue sections obtained from healthy feet of horses in the region of the DSIL-DDFT insertion on the distal phalanx (P). Panel a—Low-magnification photomicrograph of tissues obtained from a 23-year-old Dutch Warmblood did not reveal binding of safranin O dye to proteoglycan secretions. Bar = 80 µm. Panel b—Higher-magnification view of stressed tissues, revealing proteoglycan staining of cells with perinuclear cytoplasmic staining (red coloration) at the insertion site of the DSIL on the distal phalanx. Bar = 25 µm. Panel c—Photomicrograph of tissues obtained from the region of the DSIL-DDFT insertion on the distal phalanx in a 6-year-old Standardbred, revealing slight staining of proteoglycans. The tidemark is difficult to discern. Bar = 300 µm. Panel d—Photomicrograph of tissues obtained from a 6-year-old Quarter Horse, revealing moderate staining with safranin O dye and mineralized cartilage (c) in the insertion along the irregular border of the distal phalanx. Bar = 300 µm. Panel e—High-magnification photomicrograph revealing a tidemark (arrows) between the mineralized fibrocartilage insertion (c) and nonmineralized part of the DDFT and DSIL with alignment of the fibroblasts in straight lines in lacunae (arrowheads) in the nonmineralized part of the DDFT. Notice the insertion site on the bone has an irregular surface shape. Arrowheads indicate fibroblasts that stained positive for proteoglycans. Bar = 80 µm. For all panels, safranin O and fast green stains were used.

glycan staining were obtained primarily from young horses. These serial sections were from 9 horses with a mean age of 4.2 years (range, 2 to 13 years; 8 of these horses were between 2 and 6 years old). The pattern consisted primarily of perinuclear staining of isolated cells with little spread into the extracellular matrix. In the group with moderate staining, more cells that had proteoglycan staining were seen along the insertion zone of the DSIL and DDFT as well as further proximally in the DSIL-DDFT. A prominent tidemark was evident along with the extracellular staining pattern for this category (Fig 6). The graded sections in the moderate category were from 22 older horses (mean, 11.2 years; range, 4 to 21 years) that represented all breeds. More stained cells were evident along the insertion, compared with that of the first category. Only 1 horse (a 4-year-old Standardbred) was categorized as having extensive staining of the insertion. Unfortunately, a history was not available for this horse. Six horses that were > 23 years old (mean, 26 years; range, 23 to 29 years) were still being ridden at regular intervals, and tissue sections from the feet of these horses were slightly stained with a few isolated stained cells along the insertion of the DSIL and DDFT.

## Discussion

The study reported here revealed information about the DSIL-DDFT insertion on the distal phalanx in terms of macroscopic and microscopic anatomy. Results for this region were compared with results for several other ligaments in the equine foot and appeared to be more complex than those other ligaments. The DSIL-DDFT insertion consists of dense regular connective tissue fiber bundles separated by penetrating loose connective tissue septa that contain an abundance of small blood vessels, AVC, elastic tissue, and nerves. These neurovascular structures appear to be much more extensive than in other adjacent ligaments and in other areas of the DDFT. The rich innervation of the insertion and the vasculature coursing to other sites suggests a critical role in the neural control of regional tissue perfusion as well as the maintenance of proprioceptive and nociceptive functions of this area of the foot.

Additional histologic examination revealed that there was a range for proteoglycan content in the insertion of the DSIL and DDFT on the distal phalanx of healthy feet of horses. Changes in proteoglycan content may have been related to biomechanical stresses at this site as horses aged. However, in healthy feet of active horses that were in their mid-twenties, proteoglycan staining of the insertion was reduced but not that dissimilar from the staining pattern seen in the insertion of a group of younger horses. Together, these findings suggest that this variation of proteoglycan staining may be indicative of adaptive responses of these tissues and regulatory structures contained within the insertion as they continually adapt and respond to stresses applied to the foot.

The fact that the macroscopic appearance of the DSIL-DDFT insertion differed from the macroscopic appearance of other tendons or ligaments suggests that the former represent an important variation from the typical morphology of ligament and tendons and presumably is related to its function. As tendons or ligaments approach their insertion onto a bone, the structure normally becomes altered with appearance of the fibrocartilage and mineralized cartilage zones and an intervening tidemark.[11,12] The amount of fibrocartilage at the tendon insertion varies among muscles in the body. In tendons that have extensive fibrocartilage insertions, the bony insertion site is usually smooth (although not necessarily flat) and devoid of any vascular foramina, and the tendon attaches at an angle.[12] In humans, the thickness of the fibrocartilaginous zone at a tendon insertion varies and may be related to usage, with greater muscular exertion and stress of a tendon resulting in a larger zone of tendon fibrocartilage.[12] In our horses, the microscopic zone of fibrocartilage within the insertion of the DDFT and DSIL varied in thickness among feet, which may have been related to the stress of tension or compression applied by the DDFT. This observation is consistent with the

findings that the DDFT insertion on the distal phalanx is not smooth and in some horses was raised (data not shown), suggesting a response of the bone to the applied stresses at this site. Tendons that attach to a bone at an angle such as the DSIL and DDFT attachment to the distal phalanx usually have more fibrocartilage than perpendicular tendinous attachments. Such a fibrocartilage composition at the insertion serves as a protective barrier by ensuring that the tendon does not bend at the point where soft and hard tissues meet.[12] This gradual transition of the ligament and tendon to fibrocartilage and then to full mineralization in bone will alter the viscous and delayed elastic properties of the insertion to stress during movement.[11] Such a change in the physical properties of the insertion should aid in the ability of these tissues to evenly dissipate the forces and, thus, reduce the chances of failure at this site or in the DDFT.

The tendinous insertions usually do not have vascular foramina, although a small cluster of several microscopic vascular foramen are usually evident on the distal phalanx in the insertion zone of the DSIL.[13] Presumably these small foramina represent microvessel openings from the distal phalanx to the insertion. Although most ligaments and tendons have only a small to moderate vascular supply,[11,12,14] the vasculature within the insertion of the DSIL-DDFT is unique, because it also contains specialized microvessels (ie, AVC) as well as vessels that supply the navicular bone.[4]

The AVC in the DSIL-DDFT insertion resemble a glomus-type structure, rather than the direct connections of arteriovenous anastomoses between arteries and veins in the dermis of the dorsal hoof wall.[15] The arteriovenous anastomoses described in other mammals[16] may be straight or coiled, and they often possess a muscular tunic and are under sympathetic control.[14] The direct morphologic features of these cutaneous connections between the arterial and venous vessels are most often recognized as serving a thermoregulatory role[16] by maintaining the temperature of the dermal tissues at a basal set point, whereas secondarily there may be a possible contribution to the initial stages of laminitis.[2,17,18]

The location of such a tortuous capillary network suggests a potential alternative function such as sensory detection or a filtering function. During ground impact and loading, the neural network regulating the AVC and surrounding microvasculature may detect sudden pressure changes that control the patency of microvascular beds that maintain an adequate blood flow to and from the various vascular networks coursing through this region. Any pressure changes in this zone during loading could alter or potentially restrict the blood flow, or both, to most other foot regions. Such a sensory detector function would ensure adequate arterial flow to the navicular bone and distal phalanx and maintain proper venous drainage from these regions and the palmar aspect of the foot for energy dissipation.[19]

Another possible function of these AVC is maintenance of the optimal hydration of the DSIL and DDFT.[20] Such proper hydration of these connective tissues reduces the imposed shear force, which can result in increased cellular stress under normal loads and lead to the production of proteoglycans.

Compared with other ligaments of the equine digit, the portion of the DSIL-DDFT that was in the insertion on the distal phalanx contained extensive elastic tissue situated primarily within the septa between collagen fiber bundles. Although the nuchal ligament, spinal ligaments, and large arteries contain large amounts of elastin, only scant amounts of elastin are found in most other ligaments.[21] Such an elastic fiber composition of the DSIL and CSL allows for greater movement of the navicular bone during locomotion from initial ground contact to bearing of weight and lift-off and the recoil back to preimpact position.[22,23,a] During dorsiflexion of the stance cycle, the biomechanical stresses in the DSIL and navicular bone are high, because these structures are subjected to tensile and compressive forces during this weight-loading condition. During dorsiflexion movements, the position of the DSIL at the attachment to the navicular bone can change, producing different biomechanical stresses that are applied to the navicular bone. The resiliency of the elastic tissue in these support ligaments permits the navicular bone to return to its preloaded position at the end of the stance phase. Differences in elastic tissue composition between the DSIL and DDFT also suggest that shear forces may develop, causing high stress and eventually leading to pathologic changes.[24-28]

The increased amount of proteoglycan staining seen within the insertion zone indicates that fibroblasts of the DSIL and DDFT are adapting to biomechanical stresses in this region. This adaptive response, even in healthy feet of horses, appeared to become greater as the horses aged. However, in active horses in their late twenties, such proteoglycan staining in the DSIL and DDFT was comparatively less, suggesting that age may not be the determining variable. Rather, the progressive increase in proteoglycan staining may be attributable to many stresses at this site imposed on the foot during athletic performances.

One possible contributing factor to the stress within the insertion is the finding that the navicular bone becomes a weight-bearing structure during dorsiflexion.[23] Some feet of horses may have a tissue composition capable of reducing the stress within the foot at ground impact, which may lead to reduced proteoglycan production in this region. Future studies will be needed to address this possibility. During any stress in these connective tissues, production of proteoglycans is considered a normal response when fibroblasts are subjected to altered loading.[23,28] For example, as the digital flexor tendon passes under the talus bone of the tarsal joint or navicular bone, compression loads on the tendon cause an increased but localized production of proteoglycans.[26-28] With the removal of this stress, the connective tissues gradually revert to their original composition during a period of several months.[27,28] However, information is not available regarding the potential for similar adaptive responses of proteoglycan production at the insertions of ligaments and tendons, other than those in studies[26-28] of compression.

In healthy feet of horses, stresses within the inser-

tion are probably dependent on many factors during various phases of the stance cycle. These same stresses and the ensuing adaptive responses by these tissues may become excessive in feet that have an altered conformation, thereby decreasing the biomechanical efficiency of the DSIL and DDFT. Conformations that may alter functional biomechanics of feet include a long breakover, long toe-low heel conformation, little or poor support for the cuneus ungula (ie, frog), or improper trimming and shoeing.[1,3,4] On the other hand, such stress may be reduced in this region of the insertion in horses that have good support of the palmar aspect of the foot such as thick lateral cartilages and a fibrocartilaginous digital cushion with the frog contacting the ground surface.[19]

Adaptive responses with increased proteoglycan production within the insertion can normally develop during the course of a horse's life as a performing athlete. Such stress will be minimal in feet that have good support and an efficient vascular network of the palmar aspect of the foot.[23] However, continuous or excessive stress and the adaptive response in this region may progress to eventually interfere with the normal neurovascular structures and their function within the insertion. Such deleterious changes to these protective mechanisms in the insertion will eventually become evident clinically and radiographically and be recognized as signs associated with navicular syndrome.

Finally, anatomic characteristics for the region of insertion of the DSIL-DDFT on the distal phalanx may provide an explanation for the findings reported[29] during clinical examinations performed after local injection of anesthetic into the DIP joint. Such reports indicate that the anesthetic diffuses into the navicular bursa following injection into the DIP joint and desensitizes a greater area of the foot than just the DIP joint. Although dense regular connective tissue of a joint cavity or ligament would prevent or minimize diffusion of anesthetic from the joint cavity, the septa between the DSIL and DDFT at the insertion permits the locally administered anesthetic to penetrate through these tissues and eventually diffuse into the navicular bursa. Thus, although the DIP joint would be desensitized directly by local injection of anesthetic, nerves supplying the sensory function to the DSIL-DDFT insertion, navicular bone, and other sites are located within the septa and would most likely be desensitized as the anesthetic diffuses through this connective tissue. Such desensitization effects on other regions of the foot would be evident prior to entry of the locally injected anesthetic into the navicular bursa.

[a]Willemen MA. Horseshoeing, a biomechanical analysis. Doctoral thesis, Department of General and Large Animal Surgery, Faculty of Veterinary Medicine, Utrecht University, Utrecht, The Netherlands, 1997.

## References


1. Stashak TS. Lameness. In: *Adams' lameness in horses*. Philadelphia: Lea & Febiger, 1987;486–568.

2. Pool RR, Meagher DM, Stover SM. Pathophysiology of navicular syndrome. *Vet Clin North Am Equine Pract* 1989;5:109–144.

3. MacGregor CM. Navicular disease—in search of definition. *Equine Vet J* 1989;21:389–391.

4. Meier HP. A review of investigations of etiology of navicular disease. In: Hertsch B, ed. *International symposium on podotroclosis*. Munich: FN-Verlag der Deutschen Reiterlichen Vereinigung, 1994;57–59.

5. Wright IM, Kidd L, Thorp BH. Gross, histological and histomorphometric features of the navicular bone and related structures in the horse. *Equine Vet J* 1998;30:220–234.

6. Schryver HF, Bartel DL, Langrana N, et al. Locomotion in the horse: kinematics and external and internal forces in the normal equine digit in the walk and trot. *Am J Vet Res* 1978;39:1728–1733.

7. Riemersma DJ, Bogert AJ, Jansen MO, et al. Tendon strain in the forelimbs as a functional gait and ground characteristics and in vitro limb loading in ponies. *Equine Vet J* 1996;28:133–138.

8. Lochner FK, Milne DN, Mills E. In vivo and in vitro measurement of tendon strain in the horse. *Am J Vet Res* 1980;41:1929–1937.

9. Bowker RM, Van Wulfen KK. Microanatomy of the intersection of the distal sesamoidean impar ligament and the deep digital flexor tendon: a preliminary report. *Pferdeheilkunde* 1996;12:623–627.

10. Zimny ML, St Onge M, Schutte M. A modified gold chloride method for the demonstration of nerve endings in frozen sections. *Stain Technol* 1985;60:305–306.

11. Cooper RR, Misol S. Tendon and ligament insertion. *J Bone Joint Surg* 1970;52:1–10.

12. Benjamin J, Evans EJ, Copp L. The histology of tendon attachments to bone in man. *J Anat* 1986;149:89–100.

13. Getty R. Equine osteology. In: Rosenbaum C, Goshal N, Hillmann D, eds. *Sisson and Grossman's the anatomy of the domestic animals*. Philadelphia: WB Saunders Co, 1975;294–296.

14. Williams PL, Warwick R, Dyson M, et al. Myology. In: Williams PL, Warwick R, Dyson M, et al, eds. *Gray's anatomy*. 37th ed. New York: Churchill Livingstone, 1989;563–565.

15. Molyneux GS, Haller LJ, Mogg K, et al. The structure, innervation and location of arteriovenous anastomoses in the equine foot. *Equine Vet J* 1994;26:305–312.

16. Hale AR, Burch GE. The arteriovenous anastomoses and blood vessels of the human finger. *Medicine* 1960;39:191–246.

17. Hood DM, Amoss MS, Hightower D, et al. Equine laminitis, radioisotope analysis of the hemodynamics of the foot during acute laminitis. *J Equine Med Surg* 1978;2:439–444.

18. Pollitt CC, Davies CT. Equine laminitis: its development coincides with increased sublamellar blood flow. *Equine Vet J Suppl* 1998;26:125–132.

19. Bowker RM, Van Wulfen KK, Springer SE, et al. Functional anatomy of the cartilage of the distal phalanx and digital cushion in the equine foot and a hemodynamic flow hypothesis of energy dissipation. *Am J Vet Res* 1998;59:961–968.

20. Atkinson TS, Haut RC, Attiero NJ. A poroelastic model that predicts some phenomenological responses of ligaments and tendons. *J Biomech Eng* 1997;119:400–405.

21. Williams PL, Warwick R, Dyson M, et al. Connective tissues. In: Williams PL, Warwick R, Dyson M, et al. *Gray's anatomy*. 37th ed. New York: Churchill Livingstone, 1989;62–70.

22. Riemersma DJ, van den Bogert AJ, Jansen MO, et al. Influence of shoeing on ground reaction forces and tendon strains in the forelimbs of ponies. *Equine Vet J* 1996;28:126–132.

23. Bowker RM, Atkinson PJ, Atkinson TS, et al. Effect of contact stress in bones of the distal interphalangeal joint on microscopic changes in articular cartilage and ligaments. *Am J Vet Res* 2001;62:414–424.

24. Matyas JR, Antow MG, Shrive NG, et al. Stress R governs tissue phenotype at the femoral insertion of the rabbit MCL. *J Biomech* 1995;28:147–157.

25. Giori NJ, Beaure GS, Carter DR. Cellular shape and pressure may mediate mechanical control of tissue composition in tendons. *J Orthop Res* 1993;11:581–591.

26. Vogel KG, Ordog A, Pogany G, et al. Proteoglycans in the compressed region of the human tibialis posterior tendon and in ligaments. *J Orthop Res* 1993;11:68–77.

27. Gillard G, Reilly HC, Bell-Booth PG, et al. The influence of mechanical forces on the glycosaminoglycan content of the rabbit flexor digitorum profundus tendon. *Connect Tissue Res* 1979;7:37–46.

28. Vogel KG, Koob TJ. Structural specialization in tendons under compression. *Int Rev Cytol* 1989;115:267–293.

29. Keegan KG, Wilson DA, Kreeger JM, et al. Local distribution of mepivacaine after distal interphalangeal joint injection in horses. *Am J Vet Res* 1996;57:422–431.